# Settlement and Capacity of Piles Under Large Number of Cyclic Loads

**Renpeng Chen, Chunyin Peng, Jianfu Wang, and Hanlin Wang**

**Abstract** This study reports a group of field tests on cyclically loaded piles installed in soft clay in Huzhou, China. Two 29.5 m long pipe piles were instrumented with transducers to measure the accumulated settlement at the pile-head, the pore water pressure and total pressure at the pile-soil interface, and axial load at the pile end, respectively. The major objective of the field testing is to gain a better understanding of the evolution of the pile-head settlement and the effective stress at the pile-soil interface. The results of cyclic loading tests under different combinations of static load and cyclic load are discussed with reference to changes in the pile capacity, the permanent settlement, and the radial stresses. It is found that the permanent settlement of piles can be characterized as quickly stabilized (QS), progressively developing (PD), and dramatically failed (DF) patterns. Under low-level loading (QS pattern), the pile-shaft earth pressure is nearly undisturbed, final gains in effective stress are observed due to slight dissipation of pore pressure. For intermediate-level loading (PD pattern), significant reductions in pore pressure, earth pressure, and effective stress are observed after cyclic loading. Regarding high-level loading (DF pattern), the quick accumulation of pore water pressure leads to a slight increase in earth pressure, resulting in a continuous decrease in effective stress.

**Keywords** Field testing · Cyclic loading · Long-term behaviors · Soft clay

R. Chen (✉) · C. Peng · J. Wang
Zhejiang University, Hangzhou 310058, China
e-mail: chenrp@zju.edu.cn

C. Peng
e-mail: cypeng@zju.edu.cn

J. Wang
e-mail: 21712010@zju.edu.cn

R. Chen
Hunan University, Changsha 410082, China

H. Wang
The Hong Kong Polytechnic University, Hung Hom, Kowloon, Hong Kong, China
e-mail: hanlin.wang@polyu.edu.hk



E. Tutumluer et al. (eds.), *Advances in Transportation Geotechnics IV*, Lecture Notes in Civil Engineering 166, https://doi.org/10.1007/978-3-030-77238-3_79

## 1 Introduction

The accumulated settlement of piled-embankment in high-speed railways is required to be rigorously controlled [1], especially in southeastern China where extensive soft clays are often encountered. These piles undertake not only the self-weight of the embankment but also the cyclic load induced by the moving trains. Considering the unfavorable characteristics of soft clay such as high compressibility, low strength, and low permeability, a better understanding of the cyclic behaviors of piles appears important in the design of piled-embankment. The static and cyclic loading levels, the number of cycles, and the soil characteristics affect the pile-head settlement significantly [2].

Plenty of experiments have been performed to explore the cyclic behaviors of piles under cyclic loading. Concerning sand, interesting results are reported by Poulos [2], Al-Douri and Poulos [3], Gavin and O'Kelly [4], Jardine and Standing [5], Blanc and Thorel [6], and Matos et al. [7]. In most of these studies, significant degradation in the shaft capacity was observed when the piles were subjected to limited cycles (hundreds or thousands of cycles) under large cyclic loads (the cyclic amplitude > 50% of the ultimate capacity). Concerning saturated clay, Poulos carried out model tests in reconstituted saturated clay. He found that the significant reduction in shaft friction leads to failure of the model pile (Diameter $D = 20$ mm). An analysis was proposed to predict the ultimate capacity under cyclic loading [8, 9]. Huang and Liu argue that the pile behavior remains elastic at very low cyclic loading levels, higher cyclic load level leads to more severe degradation in the pile capacity [10]. Muhammed et al. conducted cyclic loading tests on the model pile ($D = 36$ mm) in saturated clay, the pore water pressure is found to increase initially to its peak then drops gradually with the number of cycles. The shaft friction degrades at the beginning before increasing again until the end of cyclic loading [11, 12].

In general, existing studies mainly focused on model piles driven in sand under short-term loading (for hundreds or thousands of cycles), simulating the effect of waves or winds on offshore structures (the cyclic load amplitude > 50% of the ultimate capacity). However, the piled-embankment in the high-speed railways suffers long-term cyclic loadings (more than $10^4$ cycles) at small cyclic amplitudes (less than 20% of the ultimate capacity). To date, field study on cyclic behaviors of industrial piles in soft clay to large number of cycles is scarcely reported.

This study reports a program of cyclic loadings on industrial piles installed in soft clay. These piles were instrumented with pore pressure transducers (PPT), earth pressure transducers (EPT), and axial load transducers (ALT). Three loading procedures were performed on the pile in sequence: initial static loading (to obtain the initial capacity), cyclic loadings (to characterize the cyclic behaviors), and final static loading (to determine the changes in pile capacity after cyclic loadings). The soil characteristics are identified before describing the pile-head settlement. Finally, the changes in the pore pressure, the earth pressure, and the effective stress are analyzed.

# 2 Experimental Setup

## *2.1 Field Profiles*

The field testing site was a leveled ground along the Hushan Expressway in Huzhou, China. Two prestressed concrete pipe piles (Pile A and Pile B) were installed to a depth of 30 m, with a spacing of 13.2 m. Samples were collected from six drilling boreholes (to a maximum depth of 62 m) to determine basic soil properties. Two cone penetration tests (CPT1 and CPT2) and two vane shear tests (VST1 and VST2) were conducted for site investigations (see soil profile in Fig. 1). The surface layer (CL1, 0–5 m) is grayish-yellow clay of intermediate plasticity. The middle layer (CL2, 5–30 m) is grey clay of high dry strength. The bottom layer (CL3, 30–35 m) is taupe clay of low plasticity with occasional silt partings. Based on the classification standards recommended by ASTM [13], these soils (0–35 m) were identified as Lean Clay (CL). Basic physical and mechanical parameters of each layer are illustrated in Fig. 1. Intact samples from CL2 indicates a cohesion $c'_{cu}$ of 6.5 kPa and an effective friction angle $\varphi'_{cu}$ of 25.5° in consolidated-undrained triaxial tests.

Two cone penetration tests (CPT) were conducted to a depth of 35 m. CPT1 was carried out at a distance of about 35 m from Pile B while CPT2 was performed about 10 m from the same pile. The CPT results indicate a cone tip resistance $q_c$ of about 2 MPa and a sleeve friction $f_s$ of about 20 kPa. Two vane shear tests (VST1 and VST2, with a spacing of 4 m) were conducted to determine the in-situ undrained shear strength $s_u$. The ratio of the intact $s_u$ to the effective overburden stress $\sigma'_v$ appeared to stabilize with the depth, with ratios of 0.16 and 0.21 for VST1 and VST2, respectively.

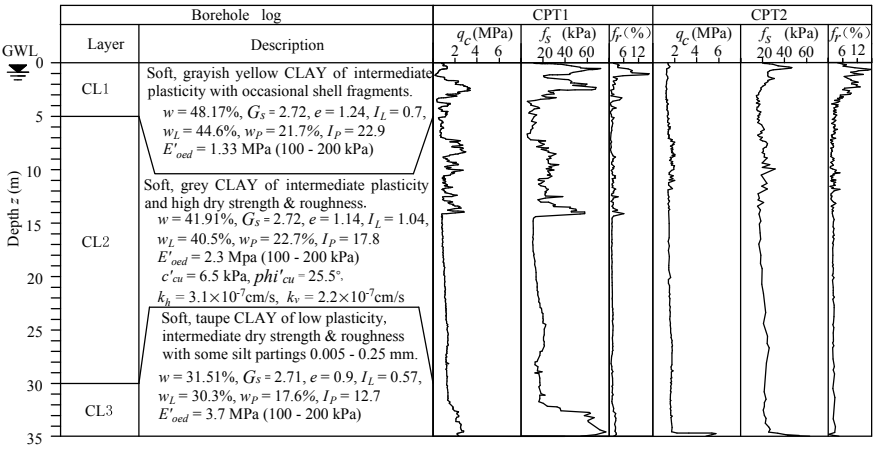


**Fig. 1** Soil profile and physical parameters of the testing site

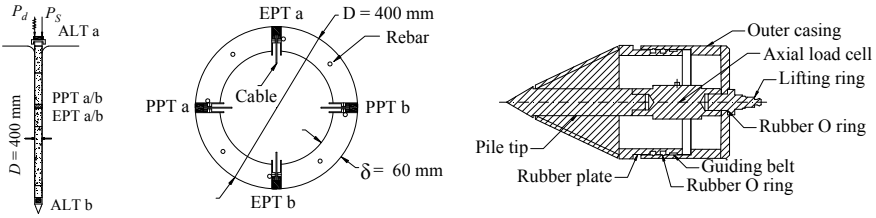


(a) Overall (b) Pile-shaft PPT and EPT (c) ALT b

**Fig. 2** The instrumentation details of transducers at the pile-shaft and the pile-end

## 2.2 Testing Preparations

The closed-ended pile had a length of 29.5 m with an outer diameter of 400 mm. Each prestressed concrete pile was instrumented with an axial load transducer (ALT a) at the pile-head to measure the applied load. Pore pressure transducers (PPT) and earth pressure transducers (EPT) were mounted at the same depth (10 m) to obtain the effective stress at the pile-soil interface. Another axial load transducer (ALT b) was designed to measure the pile-tip load. The casing of ALT b is designed to preventing smearing or inclusion of pore water or soil particles (see Fig. 2).

The testing system consisted of a reaction device, a loading device, and a measuring device. The reaction device was made up of a main reaction beam (9000 × 400 × 700 mm) and four secondary reaction beams (supported by two concrete-block cribbings and balanced by a stack of concrete blocks weighing about 1800 kN). In the loading device, the hydraulic actuator (travel: 500 mm; capacity: 1000 kN) was powered by a servo-controlled hydraulic pump. The measuring device included laser displacement transducers (LDT, independent of the loading system), axial load transducers (ALT a, ALT b), pore pressure transducers (PPT a, PPT b), and earth pressure transducers (EPT a, EPT b). All transducers were connected to a dynamic data-acquisition device reading at 100 Hz.

## 2.3 Testing Program

A series of static and cyclic loading tests were conducted on Pile A and Pile B. Three testing procedures were performed on each pile in sequence: initial static loading, cyclic loadings, and final static loading. In the initial static loading (SLA1, SLB1), the undisturbed compressive capacity of the pile was obtained, following the guidelines recommended by ASTM [14]. In the cyclic loadings, the sinusoidal loading waveform was applied as:

$$P(t) = P_s + \frac{P_c}{2}[1 + \sin(\omega t)] \quad (1)$$

**Table 1** Cyclic loading program of the field testing on Pile A and Pile B

| Procedure | Pile A | | Pile B | |
|---|---|---|---|---|
| 1 | SLA1 | | SLB1 | |
| 2 | SLR | CLR | SLR | CLR |
| | 0.01 | 0.17, 0.33, 0.44, 0.65 | 0.03 | 0.15, 0.29, 0.46, 0.57 |
| | 0.17 | 0.16, 0.24, 0.33, 0.50 | 0.16 | 0.15, 0.24, 0.31, 0.48 |
| | 0.33 | 0.08, 0.17, 0.25, 0.50 | 0.32 | 0.08, 0.16, 0.24, 0.32, 0.40, 0.48 |
| | 0.50 | 0.08, 0.17, 0.24, 0.33 | 0.48 | 0.08, 0.16, 0.24, 0.33 |
| | | | 0.64 | 0.08, 0.16 |
| 3 | SLA2 | | SLB2 | |

where $P(t)$ was the applied sinusoidal load changing with time $t$; $P_s$ was static load; $P_c$ was the peak to trough amplitude of cyclic load; $\omega$ was circular frequency. Note that the duration and rest periods in a load cycle have rarely been investigated [15]. Qiu reported that the duration of the rest period barely influence the permanent deformation of the soil in highway pavements at low load frequency [16], Liu and Xiao hold the same argument [17]. Therefore, a continuous sinusoidal wave without intervals was applied in this study. The static load ratio (SLR $= P_s/P_u$, $P_u$ is the ultimate capacity) and the cyclic load ratio (CLR $= P_c/P_u$) were defined to evaluate the loading characteristics. As indicated in Table 1, sixteen cyclic loading combinations were performed on Pile A. The SLR was 0.01, 0.17, 0.33, and 0.50, respectively, with CLR ranging from 0.08 to 0.67. Twenty similar cyclic loadings were conducted on Pile B. Each cyclic combination was terminated either after a maximum number of 50,000 cycles or reaching failure, with loading frequency ranging from 0.3 to 3 Hz depending on the loading system performance. Another static loading test was conducted on the pile (SLA2, SLB2) after cyclic loadings.

## 3 Results and Discussions

### *3.1 Pile Compressive Capacity*

The settlement required for failure is defined as 20 mm (about 5% $d$, $d$ is the pile diameter). The initial capacities of Pile A and Pile B are 490 kN and 510 kN, respectively. These two piles were subjected to 16 and 20 different cyclic loadings (see Table 1) before conducting final static loadings (SLA2, SLB2). The static compressive capacities for Pile A and Pile B increase by 22% and 24%, respectively. Both the shaft friction and the base resistance are improved.

### 3.2 Pile Head Settlement

The permanent settlement of piles under long-term cyclic loadings can be characterized as three patterns: quickly stabilized (QS), progressively developing (PD), and dramatically failed (DF). Note that the permanent settlement $s$ is obtained as the mean value of the peak $s_p$ and the trough $s_t$ in a settlement waveform.

Figure 3a shows a typical curve of quickly stabilized (QS) settlement against time. The pile-head settlement increased to 3 mm when the pile was loaded to 225 kN from 10 kN. The settlement remained horizontal or even reduced slightly during the cyclic loading period. After the termination of cyclic loading (unloaded back to 10 kN), the pile-head settlement tended to rebound to the previous position. Figure 3b illustrates three typical curves of normalized settlement $s/d$ of quickly stabilized (QS) pattern. In these three tests, the permanent settlement presented similar stable trends. In terms of quickly stabilized (QS) pattern, only negligible settlements were observed under cyclic loading over a very large number of cycles ($s < 1\%D$ in $5 \times 10^4$ cycles). Summarizing the loading conditions of quickly stabilized (QS) pattern, there exists a critical combination below which the pile-head settlement remains nearly undisturbed: CLR $\leq$ 0.2 (0 < SLR $\leq$ 0.2) or 10SLR + 5CLR $\leq$ 6 (0.2 < SLR $\leq$ 0.6).

Figure 4a indicates the typical test result of progressively developing (PD) pattern. An initial settlement of 3 mm was caused when the pile was loaded to 250 kN. As the cyclic loading (ranging from 200 to 300 kN) proceeded, the settlement kept increasing with a final peak settlement of 5 mm. Nevertheless, no failure was observed until the end of the cyclic loading. Figure 4b illustrates three normalized settlement curves of progressively developing (PD) pattern. The permanent displacement accumulated progressively with the number of cycles in the semi-log coordinates. This trend continued developing without reaching failure till the end of cyclic loading ($0.1\%D \leq s < 5\%D$ in $5 \times 10^4$ cycles). Concerning progressively developing (PD) pattern,

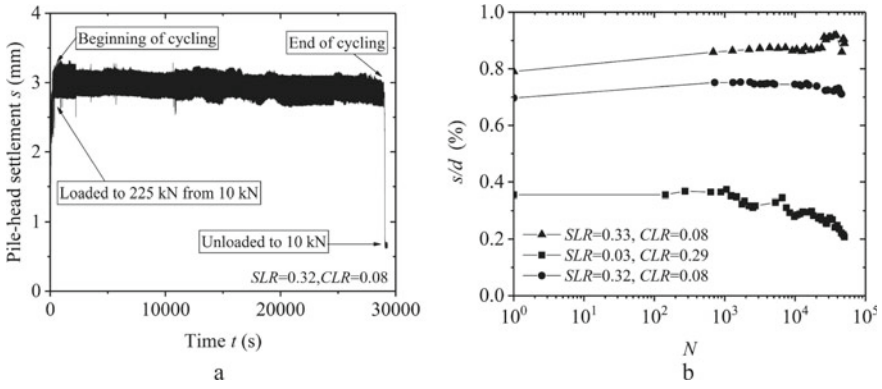


**Fig. 3** Typical QS pile-head settlement against: **a** time; **b** number of cycles

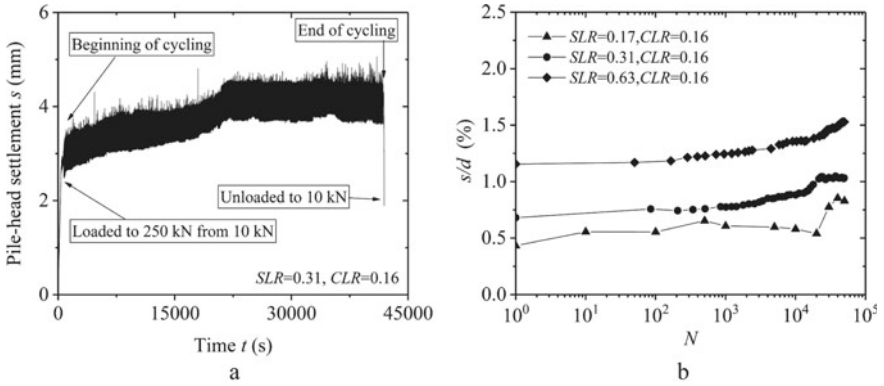


**Fig. 4** Typical PD pile-head settlement against: **a** time; **b** number of cycles

there is a upper limit under which the settlement keeps increasing without failing: $0.2 < \mathrm{CLR} \leq 0.5$ ($0 \leq \mathrm{SLR} \leq 0.2$) or $5\mathrm{SLR} + 8\mathrm{CLR} \leq 5$ ($0.2 < \mathrm{SLR} \leq 1$).

Figure 5a presents the typical displacement behavior of dramatically failed (DF) pattern. Prior to cycling, a downward movement of 4 mm was induced when the pile head was statically loaded to 350 kN. In the cyclic loading period (ranging from 200 to 500 kN), the pile-head settlement increased significantly with the number of cycles. Cyclic failure was triggered after 5000 s (about 1300 cycles) with a settlement of 23 mm. After a pause of 6 h, the pile was cyclically loaded again with the same load combination, the settlement reached 34 mm after 3200 cycles. Figure 5b shows typical normalized settlements of dramatically failed (DF) pattern. The pile-head settlement developed dramatically with the number of cycles in the semi-log coordinates, reaching failure at hundreds or thousands of cycles ($s > 1\%D$ in $10^4$ cycles or $s > 5\%D$ in $5 \times 10^4$ cycles). Concerning dramatically failed (DF) pattern, there is a lower limit above which the pile-head settlement accumulates significantly,

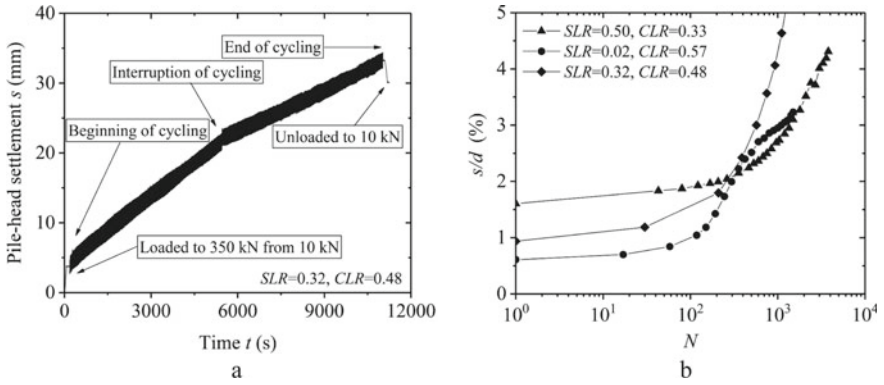


**Fig. 5** Typical DF pile-head settlement against: **a** time; **b** number of cycles

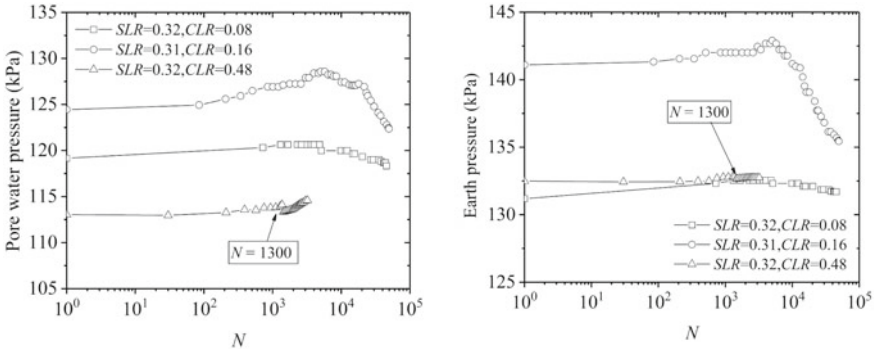


(a) changes in pore pressure (b) changes in earth pressure

**Fig. 6** The variations in pile-shaft pore water pressure and earth pressure

plunging failures are observed within limited loading cycles (generally thousands of cycles): CLR > 0.5 ($0 \leq$ SLR $\leq 0.2$) or 5SLR + 8CLR > 5 ($0.2 <$ SLR $\leq 1$). Note that the cyclic loading level (CLR) plays a dominant role in determining the settlement patterns of piles under different cyclic loading conditions. In general, if the settlement is required to be rigorously controlled, the total load applied at the pile-head is suggested to be controlled as CLR < 0.2 or 10SLR + 5CLR $\leq 6$. In order to prevent significant settlement or plunging failure, the total load is suggested to be controlled as $0.2 <$ CLR $\leq 0.5$ or 5SLR + 8CLR $\leq 5$.

## *3.3 Pile Shaft Stress*

The pore pressure and earth pressure at the pile-soil interface during cyclic loadings were obtained from transducers instrumented along the pile shaft (see Fig. 6). Under low-level cyclic loading (quickly stabilized QS pattern), the pore pressure increases slightly at early stages and then decreases gradually, indicating that the effects of cyclic loading can be neglected. In terms of intermediate-level loading (progressively developing PD pattern), the pore pressure increases significantly at early stages due to partly blocked horizontal drainage channels caused by plastic cyclic shearing on the pile-shaft clay. The pile-soil system is subsequently disturbed by long-term cyclic loading, stronger dissipation through vertical drainage chennels results in a significant reduction in pore pressure. For high-level loading (dramatically failed DF pattern), the horizontal drainage channels are quickly blocked by severe shear contraction, prompting a continuous increase in the pore pressure.

As indicated in Fig. 6b, the earth (total) pressure under low-level loading (quickly stabilized QS pattern) is nearly undisturbed by cyclic loadings, since the cyclic loading appears elastic (no significant accumulation of plastic deformation). For intermediate-level loading (progressively developing PD pattern), the earth

pressure increases slightly before reducing significantly below the initial value. Regarding high-level loading (dramatically failed DF pattern), the earth pressure keeps increasing due to the continuous accumulation of pore water pressure.

Figure 7a shows the variations of effective stresses under different cyclic loading. The effective stress under low-level loading (quickly stabilized QS pattern) obtains final gains after cyclic loading, indicating an enhancement in the pile-soil stiffness. For intermediate-level loading (progressively developing PD pattern), the effective stress decreases below the initial value despite some recovery occurs at the end of the cyclic loading, suggesting degradation of the pile-soil stiffness. The pile shaft effective stress decrease continuously under high-level loading (dramatically failed DF pattern), the loss of effective stress keeps developing with the number of cycles. As the pore water pressure accumulates, the pile-shaft effective stress drops accordingly.

Figure 7b illustrates the changes in the base resistance of piles under different cyclic loadings. For piles under low-level loading (quickly stabilized QS pattern), the pile tip resistance tends to decrease with the number of cycles. As the effective stress obtains final gains at the end of cyclic loading (see Fig. 7a), the shaft friction undertakes more axial load. Therefore, the base resistance decreases with the number of cycles. Concerning intermediate-level loading (progressively developing PD pattern), the pile shaft friction reduces slightly due to the decrease in effective stress. The base resistance increases as a result of axial load redistribution. For high-level loading (dramatically failed DF pattern), the pile-soil system is severely damaged by cyclic shearing, the decrease in effective stress leads to degradation in shaft friction. Therefore, the base resistance increases significantly due to axial load redistribution. Piles under higher cyclic loads (CLRs) lead to more obvious improvements in base resistance.

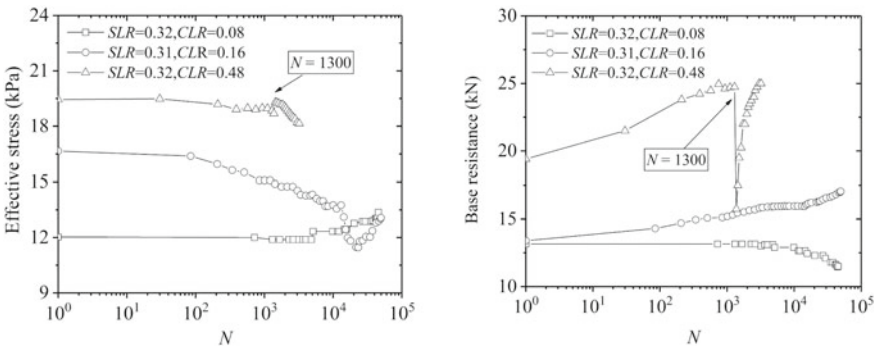


(a) changes in effective stress (b) changes in base resistance

**Fig. 7** Variations in effective stresses and base resistance

## 4 Conclusions

This study investigates the long-term behaviors of piles under different combinations of cyclic loading. The piles are instrumented with various transducers, allowing the pile-head settlement, the pore water pressure and the earth pressure at the pile-soil interface, and the pile-end axial load to be measured. Three loading procedures are applied in sequence: initial static loading, cyclic loadings, and final static loading. The variations of effective stress at the pile-soil interface and the base resistance are analyzed.

The permanent settlement of piles under cyclic loading can be characterized as three patterns: quickly stabilized (QS), progressively developing (PD), and dramatically failed (DF). Under low-level loading ($CLR \leq 0.2$ or $10SLR + 5CLR \leq 6$), the permanent settlement is negligible, the effects of cyclic loading can be neglected. Regarding intermediate-level loading ($0.2 < CLR \leq 0.5$ or $5SLR + 8CLR \leq 5$), the settlement keeps developing without reaching failure, higher cyclic load leads to larger pile-head settlement. Concerning high-level loading ($CLR > 0.5$ or $5SLR + 8CLR > 5$), the pile-head settlement develops dramatically, plunging failure occurs.

The stresses at the pile-soil interface present varied responses under different loading conditions. For low-level loading, the earth pressure is nearly undisturbed, the dissipation of pore pressure leads to final gains in effective stress. The base resistance decreases due to enforcement in shaft friction. For intermediate-level loading, the earth pressure and the pore pressure obtain initial growth before decreasing at later stages of the cyclic loading. The pile-soil system is damaged gradually, resulting in a progressive loss in effective stress. The shaft friction degrades with the number of cycles, prompting an increase in the base resistance. In terms of high-level loading, the pronounced damage in drainage channels leads to a quick accumulation of the pore pressure, the decrease in the effective stress leads to a significant degradation in the shaft friction, the base resistance increases with the number of cycles as a result of axial load redistribution.

**Acknowledgements** Support from the Hunan Provincial Science and Technology Department (Grant No. 2019RS1030) is acknowledged. The authors express their appreciation to professorate senior engineer Zhenghui Jiang from Zhejiang Institute of Communications CO., LTD for providing the testing site. The help with the experiments from Mr. Yong Xu and Dr. Wei Cheng from the Geotechnical Institute of Zhejiang University is also acknowledged.

## References

1. Wang HL, Cui YJ, Lamas-Lopez F, Dupla JC, Canou J, Calon N, Saussine G, Aimedieu P, Chen RP (2018) Permanent deformation of track-bed materials at various inclusion contents under large number of loading cycles. J Geotech Geoenviron Eng 144(8):04018044
2. Poulos HG (1989) Cyclic axial loading analysis of piles in sand. J Geotech Eng 115(6):836–852
3. Gavin KG, O'Kelly BC (2007) Effect of friction fatigue on pile capacity in dense sand. J Geotech Geoenviron Eng 133(1):63–71

4. Al-Douri RH, Poulos HG (1995) Predicted and observed cyclic performance of piles in calcareous sand. J Geotech Eng 121(1):1–16
5. Jardine RJ, Standing JR (2012) Field axial cyclic loading experiments on piles driven in sand. Soils Found 52(4):723–736
6. Blanc M, Thorel L (2016) Effects of cyclic axial loading sequences on piles in sand. Geotech Lett 6(2):163–167
7. Matos R, Pinto P, Rebelo C, Veljkovic M, Simões Da Silva L (2018) Axial monotonic and cyclic testing of micropiles in loose sand. Geotech Test J 41(3):526–542
8. Poulos HG (1980) Development of an analysis for cyclic axial loading of piles. Numer Meth Geomech 4:1513–1530
9. Poulos HG (1981) Some aspects of skin friction of piles in clay under cyclic loading. Geotech Eng 12(1):1–17
10. Huang M, Liu Y (2015) Axial capacity degradation of single piles in soft clay under cyclic loading. Soils Found 55(2):315–328
11. Muhammed RD, Canou J, Dupla JC, Tabbagh A (2018) Evaluation of local soil-pile friction in saturated clays under cyclic loading. Soils Found 58(6):1299–1312
12. Muhammed RD, Canou J, Dupla JC, Tabbagh A (2019) Evaluation of local friction and pore-water pressure evolution along instrumented probes in saturated clay for large numbers of cycles. Can Geotech J 56(12):1953–1967
13. ASTM (2017) Standard practice for classification of soils for engineering purposes (Unified Soil Classification System). American Society for Testing and Materials, West Conshohocken, PA, USA
14. ASTM (2013) Standard test methods for deep foundations under static axial compressive load. American Society for Testing and Materials, West Conshohocken, PA, USA
15. Li D, Selig ET (1994) Resilient modulus for fine-grained subgrade soils. J Geotech Eng 120(6):939–957
16. Qiu YJ (1998) Permanent deformation of subgrade soils: laboratory investigation and application in mechanistic-based pavement design. Ph.D. Thesis, University of Arkansas, Ann Arbor
17. Liu J, Xiao J (2010) Experimental study on the stability of railroad silt subgrade with increasing train speed. J Geotech Geoenviron Eng 136(6):833–841